POINT DEFECTS IN FeAl Σ5[210](-1-20) GRAIN BOUNDARY; A FIRST PRINCIPLES STUDY

Touko Lehenkari
2504313
Bachelor's Thesis
University of Oulu
Department of Physics
Spring 2020

Contents

1 Preface

With the theory of quantum mechanics have we finally truly begun to understand the inner functionalities of matter. Even despite the sheer impossibility of actually solving advanced quantum mechanical systems analytically, we are able to come into computational results thanks to the Nobel worthy work of Kohn, Sham and Hohenberg. Their density functional theory (DFT) has revolutionized computational material physics, still increasing in popularity among researchers annually to this day. For understanding many key properties of matter in different fields, the quantum mechanical aspect is necessary. Through DFT physicists, chemists and engineers alike have benefited greatly.

This thesis is a study of FeAl; an intermetallic compound which holds much promise in multiple industries due to it's high strength, excellent resistance to oxidation as well as corrosion, also having a relatively low density. However, the addition of Al content into Fe also gives rise to a new challenges, such as poor ductility in room temperature, lack of strength in higher temperatures and embrittlement of the material in the presence of water vapour, all limiting the commercial use of FeAl. [2]

Strength of FeAl is the focal point of this thesis, therefore we try to understand the mechanisms leading to eventual structural failure. We shall set our attention to the grain boundaries (GB) of FeAl, where the formation of defects can take place and create a favourable environment for a crack between the grains under stress. Two kinds of defects will be considered in this study; vacancies and hydrogen.

Vacancies have been reported to be prevalent in FeAl, increasingly so with higher temperature. They have been seen to play a major role in the strength of FeAl. With increased number of vacancies, the yield strength of bulk material of 60% iron 40%aluminum has been reported to increase in room temperature. [2] We therefore expect similar results in the presence of only vacancies, in our case they should form pretty easily in the GB.

The previously mentioned effect of water vapor weakening has been assigned to reaction water has in contact with FeAl: $3H_2O + 2Al \rightarrow Al_2O_3 + 6H$ producing a remarkable amount of hydrogen. Thanks to its minuscule size, H can infiltrate the bulk material. Its been reported to induce cracking under stress. [2] We shall introduce singular hydrogens in the grain boundary and study the interplay between them and the vacancies. The question to be answered here is: do the vacancies enable or inhibit the formation of hydrogen?

The main mission of this thesis is to shed light on the grain boundary embrittlement of FeAl via defects of vacancies and hydrogen by the means of first principles calculations. We will consider defects forming into the grain boundary by the means of calculating formation energies. [10] We shall dwell into the strength of the grain boundary by cohesive energies [11] and discussing the density of states [12] in presence of defects. A short literature review is included to consider other research regarding the topic. All the calculations done, use the Vienna *Ab initio* Simulation Package (VASP). [1] Before going into actual calculations, I will briefly go through some basic theory of DFT to validify the results acquired from the calculations themselves. Latter part of the thesis is dedicated

to discussing the results and the possible conclusions that can be drawn from them.

This thesis is a part of a wider study being conducted by myself, S. Assa Aravind, Wei Cao, Matti Alatalo and Marko Huttula at the NANOMO research unit at the University of Oulu. I would like to thank everyone for making this thesis possible.

2 Literature review

To understand the motivation behind the study at hand as well as provide further reading, we shall delve briefly into the other research regarding the topics of grain boundaries, hydrogen solubility, defects and similar *ab initio* studies.

In a study by Gang Lu and Nicholas Kioussis [14] the interaction of vacancies in a tilt grain boundary was studied by the means of first principle calculations for aluminum. Vacancies were found to most likely form in the vicinity of the grain boundary, rather than in the bulk, but not directly in the boundary plane.

Ab initio calculations of FeAl were conducted in the study of boron defects in the $\Sigma(310)[001]$ grain boundary by J. M. Raulot et al. [15]. Boron was found to be metastable in the bulk and segregate into the grain boundary substituting both Fe and Al.

Z. R. Xu and R. B. McLellan [16] heated polycrystalline FeAl of stoichiometric composition to high temperatutes with contact to H_2 gas. The solubility of H into FeAl was measured using the hot extraction process. H-atoms indeed entered the crystal occupying both tetra- and octahedral positions. The Interaction of H and point defects was not considered however.

In a very thorough article by Guikai Zhang et al. [17], theoretical *ab initio* study of B2 FeAl was conducted where H was introduced in the bulk with Fe vacancy defects. It was found that hydrogen enhances the formation of Fe vacancies in the material. Fe vacancies attract H from the bulk and can hold complexes of H within them, $V_{Fe}H_6$ being the most prevalent in ambient conditions. These complexes can still grow in size and it was suggested that this might eventually form bubbles of H_2 and induce cracking.

The energies of 408 distinct grain boundaries of bcc Fe and Mo were were calculated by embedded atom simulation techniques in a study conducted by Sutatch Ratanaphan et al. [18]. The energies of the boundaries in these two different metals correlated strongly. The boundary with the lowest boundary energy was found to be that of $\Sigma 3$ coherent twin.

In a study by Miroslav Čák, Mojmír Šob and Jürgen Hafner [19] the magnetism of two grain boundaries was studied using ab initio calculations. The grain boundaries in this study were of bcc Fe $\Sigma 5(310)$ and fcc Ni$\Sigma 5(210)$. Interstitial as well as substitutional defects of Si and Sn were added to the fully relaxed boundaries. The local magnetic moment in Fe was found to be increased compared to the bulk int the pristine case, reduced

with substitutional Sn defects and remain the same with substitutional Sn defects. The interstitial defects did not affect the magnetic moment in the boundary, but in the second and the third layers. It was wound that Si was more prone to substitutional segregation and Sn to interstitial segregation to the grain boundary.

The cohesive, magnetic and structural properties of two different grain boundaries $\Sigma 3(111)$ and $\Sigma 5(210)$ of pure bcc Fe and dillute FeCr alloy were studied in a DFT first principle calculations.In this study by E. Wachowicz, T. Ossowski, and A. Kiejna [20], the relaxation of the $\Sigma 5(210)$ revealed a substantial parallel shift between the grains. The Cr impurities segregated into the grain boundaries as well.

In the spectroscopical study by S. Gialanella [21] B2 FeAl of different Al contents was exposed to water vapor and high temperatures. The most dominant encountered defect was determined by the temperature and the amount of Al. Larger defects were detected in the microcracks mainly along grain boundaries, suggesting a big role played by the grain boundaries in the macroscopic properties of the material.

In the Edvard DeMille Cambell memorial lecture 2014 [22], numerous different mechanisms of hydrogen embrittlement are reviewed from the perspective of in-situ research.

MSE 5317-wiki is a website upheld by term papers done by students involved in material science and engineering [23]. An article page on the topic of hydrogen embrittlement provides a general overview on the topic and some research on the topic is reviewed with detail. The embrittlement due to hydrogen diffusion into the bulk of the material is not a problem only unique to FeAl, but to most metals. The metals not usually affected by this are copper, gold and tungsten.

3 Theory

3.1 Schrödinger equation of a lattice

Let us first consider any kind of lattice making up condensed matter in the macro scale. It consists of only electrons and nuclei. This system is the root of our problem and the beginning point of everything of what is about to follow.
The quantum mechanical description of a time independent system can be written using the Schrödinger equation of the form:

$$\hat{H}\left|\psi\right\rangle = E\left|\psi\right\rangle, \tag{3.1}$$

where the wave function of the system in question consisting of nuclei and electrons is of the form:

$$\psi(\{\mathbf{R}_i\}, \{\mathbf{r}_j\}).$$

Here $\mathbf{R}_i$ represents the coordinates of nuclei $0 \leq i \leq N_{nuc}$ and $\mathbf{r_j}$ represents the coordinates of the electrons $0 \leq j \leq N_{el}$, respectively. E is the total energy of the whole system and the hamiltonian operator is:

$$\hat{H} = \hat{T}_{nuc} + \hat{T}_{el} + \hat{V}_{nuc} + \hat{V}_{el} + \hat{V}_{nuc-el}. \tag{3.2}$$

The first and the second terms describe the kinetic energy of the nuclei and electrons:

$$\hat{T}_{nuc} = -\sum_{i}^{N_{nuc}} \frac{\hbar^2}{2M_i}\nabla^2_{\mathbf{R}_i}, \hat{T}_{el} = -\sum_{j}^{N_{el}} \frac{\hbar^2}{2m_e}\nabla^2_{\mathbf{r}_j}. \tag{3.3}$$

The third and the fourth terms are the potential energy between the same type of particles due to the Coulomb interaction:

$$\hat{V}_{nuc} = \frac{1}{4\pi\epsilon_0}\sum_{i\neq j}^{N_{nuc}} \frac{Z_i Z_j e^2}{|\mathbf{R}_i - \mathbf{R}_j|}, \hat{V}_{el} = \frac{1}{4\pi\epsilon_0}\sum_{i\neq j}^{N_{el}} \frac{e^2}{|\mathbf{r}_i - \mathbf{r}_j|}. \tag{3.4}$$

The last term of the hamiltonian, as one might expect is the potential energy between different kinds of particles due to the coulomb interaction:

$$\hat{V}_{nuc\leftrightarrow el} = -\frac{1}{4\pi\epsilon_0}\sum_{i}^{N_{nuc}}\sum_{j}^{N_{el}} \frac{Z_i e^2}{|\mathbf{R}_i - \mathbf{r}_j|}. \tag{3.5}$$

The problem described above, while somewhat reasonable in theory, becomes utterly impossible when trying to solve it analytically for systems with multiple particles. In fact only three systems in the history of quantum mechanics have been solved without assumptions: infinite potential well, two state system and the hydrogen atom. To reach any physical model for just about anything else under the conditions of quantum mechanics, one must make assumptions to go further.

To reduce the complexity of the many body problem, we first make the Born-Oppenheimer approximation, which states that the electrons in the system can be treated separate from the nuclei. In other words the nuclei shall be represented as fixed points in space while the electrons adjust to the potential of their making. This crude sounding approximation is thought to be reasonable, the masses of the electrons being minuscule compared to that of the nuclei.
The many body wave function can the be written as the product of the electron- $(\psi_{nuc}^{\{\mathbf{R}_i\}}(\mathbf{R}_i))$ and the nuclei parts $(\psi_{nuc}(\mathbf{r}_j))$, which could be solved separately. Our wave function is now represented as:

$$\Psi(\{\mathbf{R}_i\},\{\mathbf{r}_j\}) = \psi_{nuc}^{\{\mathbf{R}_i\}}(\mathbf{R}_i)\,\psi_{nuc}(\mathbf{r}_j). \tag{3.6}$$

3.2 Density functional theory

To further reduce the dimensionality of our problem all the way down to just 3 spatial coordinates $\mathbf{r} = \{r_1, r_2, r_3\}$, we shall delve into the world of density functional theory (DFT). The basic lemma described by Kohn and Hohenberg in 1964 goes as follows:

The ground state density $n_0(\mathbf{r})$ of a bound system of interacting electrons in some external potential $V_{ext}(\mathbf{r})$ determines this potential uniquely.

So in further examination of our core many body problem we shall not treat the electrons in the system as individuals, but rather as electron density $n(\mathbf{r})$ in our finite system being under an external potential $V_{ext}(\mathbf{r})$, interacting with it. The properties of the system are determined by this density. For example, the energy of the system is a function of n: $E[n(\mathbf{r})]$. Since $n(\mathbf{r})$ is also function of the position, the energy is such that it maps a function to a number. This is called a functional. The functional dependency is indicated by [ ]. The following formulation is taken from the Nobel lecture by Walter Kohn. [3]

3.2.1 Hohenberg-Kohn formulation

Here we shall attempt to derive the most important property of the ground state; its energy E. Applying the Rayleigh-Ritz minimal principle to our hamiltonian H with a normalized ($\langle\Psi|\Psi\rangle = 1$) trial function $\tilde{\Psi}$ of N, a given electron density $n(\mathbf{r})$ gives the energy equation as follows:

$$E = min_{\tilde{\Psi}}\left(\tilde{\Psi}, H\tilde{\Psi}\right). \tag{3.7}$$

The correct wave function is such that it minimises the ground state energy. Multiple approaches can be used here. We shall use the constrained search method. This is carried out in two parts; first we shall set a trial density $\tilde{n}(\mathbf{r})$ with which we denote trial wave functions $\tilde{\Psi}_{\tilde{n}(\mathbf{r})}$. Then we insert those to the Rayleigh-Ritz minimal principle shown above. The second step is then taken by minimizing the acquired equation with respect to all $\tilde{n}$, finally giving us E.

The first step:

$$E_{V_{ext}}\left[\tilde{n}\left(\mathbf{r}\right)\right] \equiv \int V_{ext}\left(\mathbf{r}\right)\tilde{n}\left(\mathbf{r}\right)d\mathbf{r} + F\left[\tilde{n}\left(\mathbf{r}\right)\right]. \tag{3.8}$$

Here F stands for a universal functional; the part that does not depend on information of V_{ext} and its form is therefore the same for all electronic systems:

$$F\left[\tilde{n}\left(\mathbf{r}\right)\right] = min_{\tilde{\Psi}}\left[\tilde{\Psi}_{\tilde{n}(\mathbf{r})}, \left(T+U\right)\tilde{\Psi}_{\tilde{n}(\mathbf{r})}\right]. \tag{3.9}$$

The second step:

$$E = min_{\tilde{n}_{(\mathbf{r})}} E_{V_{ext}}\left[\tilde{n}\left(\mathbf{r}\right)\right] = min_{\tilde{n}_{(\mathbf{r})}}\left\{\int V_{ext}\left(\mathbf{r}\right)\tilde{n}\left(\mathbf{r}\right)d\mathbf{r} + F\left[\tilde{n}\left(\mathbf{r}\right)\right]\right\}. \tag{3.10}$$

The original problem of the many body Schrödinger equation has now been reduced to just this; finding a minimum of $E_{V_{ext}}\left[\tilde{n}\left(\mathbf{r}\right)\right]$ with respect to a three dimensional function of trial density $\tilde{n}\left(\mathbf{r}\right)$. The only remaining unknown keeping us from reaching adequate solutions is the kinetic energy term T that is associated with the said density. In many cases this uncertainty makes the results unreliable. Because of this, most modern practical methods of DFT do no use the Hohenberg-Kohn formulation. The more popular alternative shall be discussed in the next section.

3.2.2 Kohn-Sham equations

The main goal of this section is to establish an iterative self consistent method to approximate the ground state of a system for a system of interacting electrons. This has been done in the form of so called Kohn-Sham equations. The universal functional (3.9) is now written in the form:

$$F\left[\tilde{n}\left(\mathbf{r}\right)\right] = T_s\left[\tilde{n}\left(\mathbf{r}\right)\right] + \frac{1}{2}\int\frac{\tilde{n}\left(\mathbf{r}\right)\tilde{n}\left(\mathbf{r}'\right)}{\left|\mathbf{r}-\mathbf{r}'\right|}d\mathbf{r}d\mathbf{r}' + E_{xc}\left[\tilde{n}\left(\mathbf{r}\right)\right]. \tag{3.11}$$

Inserting this $F\left[\tilde{n}\left(\mathbf{r}\right)\right]$ into the Hohenberg-Kohn variational principle (3.8) yields:

$$E_{V_{ext}}\left[\tilde{n}\left(\mathbf{r}\right)\right] = \int V_{ext}\left(\mathbf{r}\right)\tilde{n}\left(\mathbf{r}\right)d\mathbf{r} + T_s\left[\tilde{n}\left(\mathbf{r}\right)\right] + \frac{1}{2}\int\frac{\tilde{n}\left(\mathbf{r}\right)\tilde{n}\left(\mathbf{r}'\right)}{\left|\mathbf{r}-\mathbf{r}'\right|}d\mathbf{r}d\mathbf{r}' + E_{xc}\left[\tilde{n}\left(\mathbf{r}\right)\right] \geq E. \tag{3.12}$$

Here the third term describes potential due to classical coulomb interaction between the electron densities. $T_s\left[\tilde{n}\left(\mathbf{r}\right)\right]$ stands for kinetic energy of the ground state of electrons in the noninteracting case corresponding to the density distribution of $\tilde{n}\left(\mathbf{r}\right)$.
The last term $E_{xc}\left[\tilde{n}\left(\mathbf{r}\right)\right]$ is perhaps the most peculiar. Known as the exchange-correlation functional, it will require deeper understanding and will be properly discussed in the next section.
The Euler-Lagrange equations for (3.12), considering that the system does not variate with respect to $\tilde{n}\left(\mathbf{r}\right)$ (the number of electrons in the system stays the same) is then:

$$\delta E_{V_{ext}}\left[\tilde{n}\left(\mathbf{r}\right)\right]=\int\delta\tilde{n}\left(\mathbf{r}\right)\left\{V_{eff}\left(\mathbf{r}\right)+\frac{\delta}{\delta\tilde{n}\left(\mathbf{r}\right)}T_{s}\left[\tilde{n}\left(\mathbf{r}\right)\right]\mid_{\tilde{n}(\mathbf{r})=n(\mathbf{r})}-\epsilon\right\}d\mathbf{r}=0. \tag{3.13}$$

Here $V_{eff}\left(\mathbf{r}\right)$ is defined as:

$$V_{eff}\left(\mathbf{r}\right)\equiv V_{ext}\left(\mathbf{r}\right)+\int\frac{n\left(\mathbf{r}'\right)}{\left|\mathbf{r}-\mathbf{r}'\right|}d\mathbf{r}'+V_{xc}\left(\mathbf{r}\right), \tag{3.14}$$

where the last term corresponds to the exchange-correlation potential is:

$$V_{xc}\left(\mathbf{r}\right)\equiv\frac{\delta}{\delta\tilde{n}\left(\mathbf{r}\right)}E_{xc}\left[\tilde{n}\left(\mathbf{r}\right)\right]\mid_{\tilde{n}(\mathbf{r})=n(\mathbf{r})}. \tag{3.15}$$

The potential $V_{eff}\left(\mathbf{r}\right)$ now has a different form from the case of noninteracting electrons, but the form of equation (3.13) is otherwise identical to what one might get applying the methods of section (3.2.1) to the noninteracting case. Therefore we can conclude that the solution that minimizes $n\left(\mathbf{r}\right)$ is the same one that solves the single particle equation:

$$\left(-\frac{1}{2}\nabla^{2}+V_{eff}\left(\mathbf{r}\right)-\epsilon_{j}\right)\varphi_{j}\left(\mathbf{r}\right)=0, \tag{3.16}$$

where we recall the effective potential as:

$$V_{eff}\left(\mathbf{r}\right)\equiv V_{ext}\left(\mathbf{r}\right)+\int\frac{n\left(\mathbf{r}'\right)}{\left|\mathbf{r}-\mathbf{r}'\right|}d\mathbf{r}'+V_{xc}\left(\mathbf{r}\right), \tag{3.17}$$

while the density is the acquired single particle equations:

$$n\left(\mathbf{r}\right)=\sum_{j=1}^{N}\left|\varphi_{j}\left(\mathbf{r}\right)\right|^{2}. \tag{3.18}$$

The three equations above $(3.16-18)$ are known as the self consistent Kohn-Sham equations. The self consistency is defined in such a way that one can start with an initial guess for the density $n\left(\mathbf{r}\right)$ (a trial density), insert that into equation (3.16) and acquire V_{eff}, then proceed to solve the single particle equations (3.18), closing the cycle by acquiring a new elecron density $n\left(\mathbf{r}\right)$. One keeps iterating until the density converges to an acceptable degree. This way, one might finally calculate the ground state energy for a system with interacting electrons:

$$E=\sum_{j}\epsilon_{j}+E_{xc}\left[n\left(\mathbf{r}\right)\right]-\int V_{xc}\left(\mathbf{r}\right)n\left(\mathbf{r}\right)dV_{ext}-\frac{1}{2}\int\frac{n\left(\mathbf{r}\right)n\left(\mathbf{r}'\right)}{\left|\mathbf{r}-\mathbf{r}'\right|}. \tag{3.19}$$

This is similar to the same equation for energy one might get in the case of noninteracting electrons, but now with one rather straightforward difference; the exchange-correlation energy $E_{xc}\left[n\left(\mathbf{r}\right)\right]$ summed within. Finally we have reached suitable solutions to our initial many body Schrödinger equation. In Kohn-Sham equations the interaction between

electrons is included in the potential, rather than the single electron wave functions, the potential is manipulated in such a way that one arrives in the same density as in the case of interacting electrons, yielding in the same physical phenomena. With a set exchange potential, the equation above will produce not an approximate, but a true solution with that defined potential. So the solution's truthfulness rests completely on this very term. It is not something one might consider similar in all occasions. Different interpretations arise in the wake of different kinds of calculations. These approximations originate from physical study of the electronic structure outside of DFT.

3.2.3 Exchange-correlation

The exchange and correlation effects are due to different phenomena, but are handy to include in the same therm. The exchange effect is due to the Pauli exclusion principle, in which electrons of different spins repel each other. The correlation effect is due to the repelling even despite having different spins. Both make up some "hole" in the density. Now that the importance and meaning of this term has been established, we shall go through the most straight forward approximation for it, known as the local density approximation (LDA) [3], finally leading us to the approximation used in the calculations of this thesis: the generalized gradient approximation (GGA). [4]
The most important approximations for the exchange correlation term have a quasilocal form:

$$E_{xc}[n(\mathbf{r})] = \int e_{xc}(\mathbf{r}; [n(\tilde{\mathbf{r}})])\, n(\mathbf{r})\, d\mathbf{r}. \tag{3.20}$$

Here $e_{xc}(\mathbf{r}; [n(\tilde{\mathbf{r}})])$ is the energy/particle at a particular point in the density distribution of $n(\tilde{\mathbf{r}})$. The most simple approximation for this density is the uniform distribution. This is the defining idea behind LDA. When we replace the density $n(\tilde{\mathbf{r}})$ with an uniform density $n(\mathbf{r})$, the equation above takes the form:

$$E_{xc}^{LDA}[n(\mathbf{r})] = \int e_{xc}(n(\mathbf{r}))\, n(\mathbf{r})\, d\mathbf{r}. \tag{3.21}$$

Despite the approximation being very crude, it has produced surprisingly accurate results. Still it does not allow for much variation in bond lengths and in the case of systems of heavy fermions; it can completely fail. It is still referred to as being the mother of all approximations. Indeed it is at least the mother of the next one.
We employ the generalized gradient approximation (GGA) for our calculations. As the name indicates, it does not only depend on the electron density, but also the gradient term is taken into consideration.

Our approximation for the exchange correlation term is known as the generalized gradient approximation (GGA). [4] Here the excange correlation energy is dependable not only from electron density $n(\mathbf{r})$, but also from its gradient as:

$$E_{xc}^{GGA}[n(\mathbf{r})] = \int d\mathbf{r} n(\mathbf{r})\, \epsilon_{xc}(n(\mathbf{r}), \nabla n(\mathbf{r})). \tag{3.22}$$

It does not have universally accepted form, or method of producing results. There are, however, many different options to choose from. We use the versatile Perdew-Burke-Ernzerhof implementation (PBE). [4] It is a vast set of rules, and conditions defining different approach in varying cases. An overview would be lengthy process and I deem it to be outside the scope of this thesis.
All in all, the most relevant observation made in these purely theoretical sections are the Kohn-Sham equations. The iterative method discussed at the end of section (3.2.2) is the basis for all the calculations made for this study. Everything else in the former sections is just a discussion of their origin, as well as their constituents.
In practice, DFT calculations are always made through computer simulations. This gives a rise to a new relevant discussion of accuracy vs. computational burden. How will one represent the particles in the system? What of their interaction? Obviously one cannot simulate the whole of macroscopic system. Then what piece of it is enough to simulate, to accurately acquire macroscopic properties of the system? Next sections shall tackle the decisions and methods that constitute the simulations performed in the study.

3.3 Computational DFT

The first principles calculations in this study were performed using the Vienna *ab initio* Simulation Package (VASP). The ultrasoft pseudopotentials [5] are taken from the plane wave psoudopotential code to represent the solid state grid formed by the nuclei. The valence electrons are then represented by the means of plane waves. The projector augmented wave method (PAW) [6] in the PBE [4] formalism has been used for the calculations and the details are presented in theory section afterwards.

The simulated cells are made of body centered cubic iron aluminum 1:1 mixture and represent the surface as well as the Σ5[210](-1-20) grain boundary. Monkhorst Pack k-grid was used to represent the reciprocal lattice. [11] All of these parameters and their chosen values are introduced briefly in this section to understand the calculations. However, many of these subjects are rather complex and surely could provide for theses of their own. Therefore the main focus here is just to identify our parameters and explore their meanings in this complex process. I see that this brief consideration is a necessary passage to connect our theory and practice.

3.4 Cell

Our bulk material has a B2 structure, where the amount of Fe is equal to Al. The grain boundary in our cell is a Σ5 [210](-1-20), grain boundary (GB) simply meaning a tilt of 36.86° between the grains in the y-z plane as seen in the figure 1 below. The lattice parameters of the shell are $(a, b, c) = (2.87250, 25.69243, 6.42311)$Å, which encapsulates 20 of both Fe and Al.
The structure above is ordered in such a way that it is not stable and not found in nature. Therefore we have relaxed it. This means a calculation where the particles in the cell are allowed to move to positions which minimize the Hellman-Feynman forces. The details of this process are referred to in the section: Relaxed cell geometry. To this structure

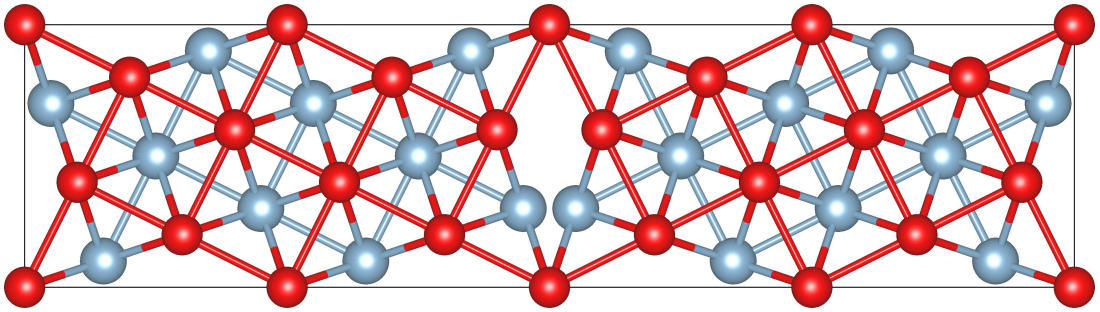

Figure 1: The unrelaxed FeAl grain boundary

we began to add point defects in further calculations. Only two types of defects occur in this study: hydrogen and vacancies. Hydrogens were placed in three different positions: in a place of an Al or a Fe atom in contact with the GB, as well as to an interstitial position replacing no particles. Two kinds of vacancies were introduced with contact to the replacements in the places of Al and Fe. The positions for each can be seen in the figure 2 below:

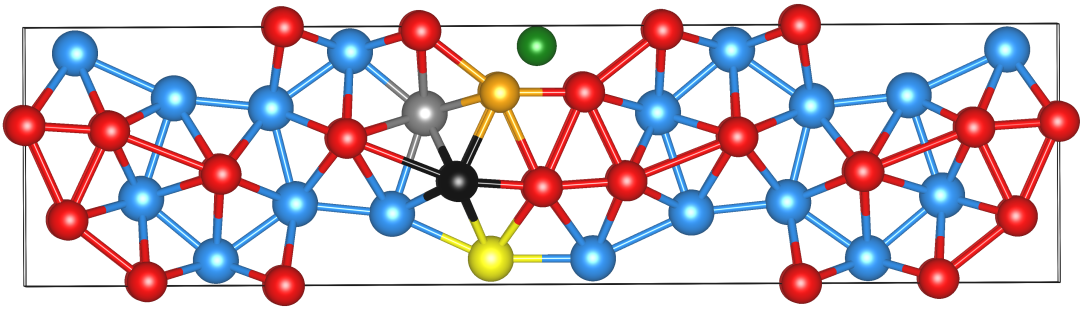

Figure 2: The relaxed FeAl grain boundary with marked in defects

Defect	Color
$H_{int.}$	Green
H_{Fe}	Orange
H_{Al}	Yellow
V_{Fe}	Black
V_{Al}	Gray

3.5 k-grid

In solid state physics a lattice can be projected from a normal position space to a momentum space. This is done with a method known as a Fourier transform and the acquired lattice is called the reciprocal lattice. Given primitive vectors for a direct three dimensional lattice $(\mathbf{a_1}, \mathbf{a_2}, \mathbf{a_3})$ the reciprocal lattice vectors can be generated as [11]:

$$\mathbf{b_1} = 2\pi \frac{\mathbf{a_2} \times \mathbf{a_3}}{\mathbf{a_1} \cdot (\mathbf{a_2} \times \mathbf{a_3})}, \mathbf{b_2} = 2\pi \frac{\mathbf{a_3} \times \mathbf{a_1}}{\mathbf{a_1} \cdot (\mathbf{a_2} \times \mathbf{a_3})}, \mathbf{b_3} = 2\pi \frac{\mathbf{a_1} \times \mathbf{a_2}}{\mathbf{a_1} \cdot (\mathbf{a_2} \times \mathbf{a_3})}. \tag{3.23}$$

The Wigner-Seitz cell (meaning the surrounding space of a lattice point that is closer to it than any other point) is called a Brilloiun zone in reciprocal lattice.

Many of the key numerical results of a solid state system cannot be be obtained without integrations over this Brilloiun zone, such as total energy, density of states and charge density, all of which require knowledge of the momentum of the particles. In computations, these integrals can be replaced with a sum over specified K-points. [7] The integrations over the first Brillouin zone generally take the form:

$$I(\epsilon) = \frac{1}{\Omega_{BZ}} \int_{BZ} d\mathbf{k} F(\epsilon) \delta(\epsilon_{n\mathbf{k}} - \epsilon) \rightarrow \sum_{\mathbf{k}} \omega_{\mathbf{k}_i} F(\epsilon) \delta(\epsilon_{n\mathbf{k}} - \epsilon). \tag{3.24}$$

Ω_{BZ} is the volume of the Brillouin zone and $\omega_{\mathbf{k}_i}$ is then the factor that conserves the volume when representing the integral as a sum. $\delta(\epsilon_{n\mathbf{k}} - \epsilon)$ is the delta function and $F(\epsilon)$ is its set value. The selection of these k-points then becomes crucial. In this study a Monkhorst-Pack scheme is used where the k-points are distributed in uniform fashion. This is a proper choice for metallic systems such as ours. Also, the step functions prevalent in these can be replaced with smoother smearing schemes. In our metallic system, we used the Methfessel-Paxton scheme. [9] Later we replace the periodic potential of a lattice with smoother potentials to represent the nuclei. It is therefore reasonable to treat the k-points in a same manner with smearing. It has been recorded to work with high precision.

3.6 Plane waves

In actual computations of DFT the wave functions of individual electrons are represented in a finite sets of functions; also known as a basis sets. In this study the system is a periodic bulk solid. Therefore a good choice are plane waves from Bloch's theorem of the form:

$$\psi_{i,\mathbf{k}}(\mathbf{r}) = \sum_{\mathbf{G}}^{|\mathbf{G}|\leq G_{max}} c_{i\mathbf{k},\mathbf{G}} e^{-(\mathbf{k}+\mathbf{G})r}. \tag{3.25}$$

The waves are orthogonal by definition and are summed over reciprocal lattice points $\mathbf{G}$. $\mathbf{k}$ is simply the wave vector in reciprocal space and $c_{i\mathbf{k},\mathbf{G}}$ are Fourier coefficients. The accuracy of this representation is dependable on the number of plane waves summed increasing the computational burden with added plane waves. The upper bound for the number of plane waves is defined via cutoff energy E_c. In our case $E_c = 450eV$. Now we can acquire G_{max}:

$$G_{max} = \frac{\sqrt{2E_c m_e}}{\hbar}. \tag{3.26}$$

3.7 Ultrasoft pseudopotentials

The description of the atomic cores as well as the electrons bound tightly to them is done by pseudopotentials. If one was to simply treat the potential of a core straight as:

$$V(r) = -\frac{Ze}{r}, \tag{3.27}$$

one would have to deal with rapid oscillations of the wave functios in the vicinity of the core. However, the chemical bonding in a lattice is mostly due to the workings of the valence electrons. This highly suggests that one could replace this steep potential with a smoother one. These potentials are known as pseudopotentials. A pseudopotential has to abide to certain restrictions. Its valence electron wave functions are to be described as:

$$R_l^{PP}(r) = R_{nl}^{AE}(r), r > r_l. \tag{3.28}$$

Here the radial pseudo wave function around the nuclei with l angular momentum $R_l^{PP}(r)$ is the same as the radial n valence electron wave function outside of the cutoff range r_l: $R_{nl}^{AE}(r)$.
Secondly, the eigenvalues of the functions have to be the same:

$$\epsilon_l^{PP} = \epsilon_{nl}^{AE}. \tag{3.29}$$

Lastly the wave functions should not have nodal surfaces, meaning areas where the probability of finding an electron is zero. With these regulations there are multiple pseudopotential methods to choose from. This study uses the first principles ultrasoft pseudopotential method [5], where the Kohn-Sham equations take the form of generalized eigenvalue equations:

$$H\phi_i = \epsilon_i S\phi_i. \tag{3.30}$$

In this study the pseudopotentials used for the nuclei are taken from the VASP library.

3.8 Projector augmented wave method

The methodology of using ultrasoft pseudopotentials along with planewaves is called the Projector augmented wave method (PAW). [6] It is a quantum mechanical operator based method. The partial wave expansions to sample the electrons are determined by the overlap with localized projector functions. All the intricacies of this theory shall not be discussed, but let us briefly go over the very basics, beginning with a linear transformation T:

$$|\psi_n\rangle = T|\tilde{\psi_n}\rangle. \tag{3.31}$$

This linear transformation maps the true electron wave functions ψ_n to our smoother plane waves $\tilde{\psi_n}$. The sub-index n in reality contains the band-, reciprocal wave vector **k**- as well as spin indices defining the wave function in question. T is localised around the nuclei in such a way, that it stops to operate outside a case specified cutoff region of a radius r_c. This transforms the Kohn-Sham equations as:

$$T^\dagger H T|\tilde{\psi_n}\rangle = T^\dagger T|\tilde{\psi_n}\rangle\epsilon_n. \tag{3.32}$$

4 Results and Discussion

With the constituents of the calculations specified and transformed into their computational forms we shall move into the results of the simulations. We shall begin with discussing the particle movement during the relaxation, then the energetics of the defects formation and lastly try to find explanations for such from electronic structure by the means of density of states.

4.1 Relaxed cell geometry

The first step of all our calculation is the relaxation of the cell. The stress tensor and the forces acting on the particles were calculated and the particles were allowed to move inside the cell of fixed shape and volume. The ionic steps were done using the conjugate gradient algorithm. [8]

Let us observe the total movement of the particles in the relaxation. This is done by simply taking the difference of positions in the unrelaxed- and the relaxed case for each particle in the vicinity of the GB. We only consider the movement of four particles in direct contact with the GB. This is sufficient because of the inherent symmetry of our GB: the other side is considered to relax the same way. I shall present this in a table form and then calculate the average particle movement in the relaxation.

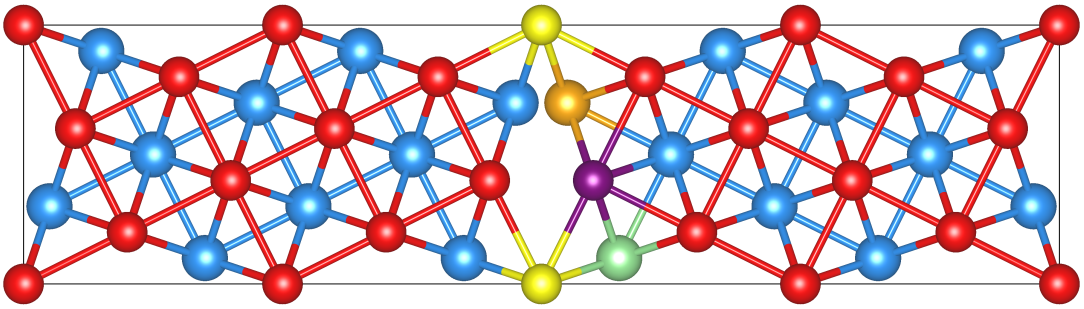

Figure 3: The unrelaxed structure with the tracked particles marked in

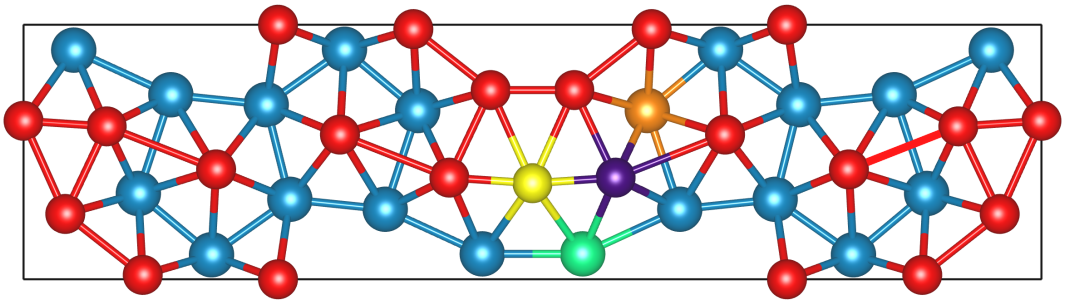

Figure 4: The relaxed FeAl grain boundary with marked in tracked particles

The movements of our particles, two of Al and Fe each, are shown here:

Particle:	Al1 (Green)	Al2 (Orange)	Fe1 (Yellow)	Fe2 (Purple)
Δx (Å)	0	0	0	0
Δy (Å)	0.65931	-2.2555	0	1.28462
Δz (Å)	0.00160	0.23790	2.42434	0.14490
total:	0.65932	2.26800	2.42434	1.29277

There is no movement in the x direction. In this direction the cell is smaller and the Fe and Al are already closely packed. The atoms of Fe and Al moved in their own y-z planes. All this is to be expected in a periodical cell such as this. Fe1 is acting as a somewhat central particle and is adjusting itself only in z direction, constantly maintaining its central position in the cell. The only particle to lose its positioning in the GB was Al2, which gave it to an Fe particle behind it.

The relaxed structure can be considered energetically stable since the free energy converged neatly with computed iterations in the calculations, until the change in energy between the iterations was within the accepted limit of $10^{-6}eV$. The GB forms peculiar ring patterns of five Al atoms.

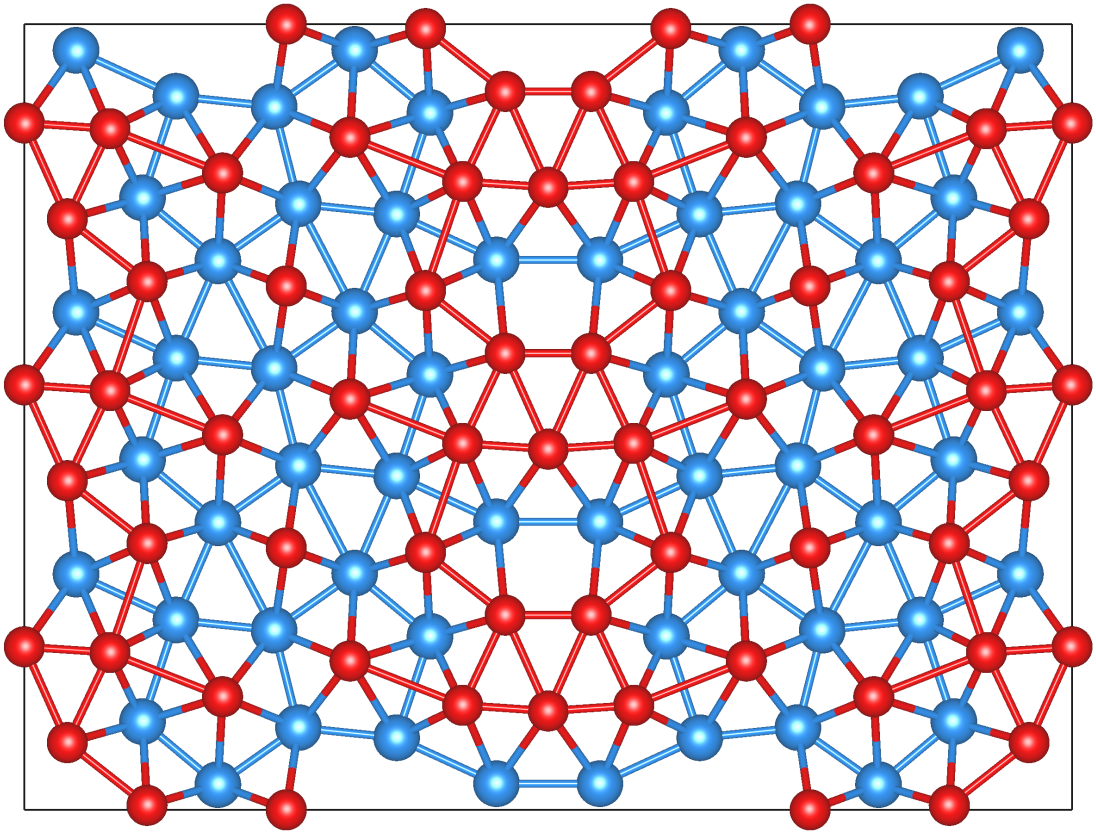

Figure 5: The relaxed FeAl grain boundary with a larger super cell

4.2 Formation energy

To have understanding about the frequency and the overall ease of defect formation in the GB we have used the method of formation energies. In other words, the energy change of the system while undergoing a formation of a defect. [10] Its given by the formula:

$$E_f(D) = \frac{E_{GB+D} - (E_{GB} - n_i\mu_i)}{n_i}. \tag{4.1}$$

Here E_{GB+D} is the total energy of the cell with the said doping and E_{GB} the energy without it. μ_i is the chemical potential of a defect installed and n_i the amount of defects added one by one. In the formula, the sign of n_i depends upon if the defect is made by adding (-) or subtracting (+) from the initial case.
Here are some tables of the constituents in the calculations. The structure for each GB can be seen in the cell section.
Total energies are acquired straight from the calculations, given by the output files for each case. Chemical potentials are the energies of a singular particle in the assigned environment. These are calculated using the super cell approach; using Fe and Al rich

environments and for each metallic article are the total free energy of the bulk, divided by the number of particles. In the case of a hydrogen it the energy required to remove it from such an environment. For each different atom in our case they are:

Element	Chem.pot(eV)
Fe	-8.25
Al	-3.65
H	-0.05675231

Here the calculated total energies of each GB system and the **formation energies** from the formula (3.2.1):

Structure	Total energy(eV)	Formation energy(eV)
Pristine	-238.22321211	0
V_{Al}	-239.98130958	-5.60809747
V_{Fe}	-235.66627292	-5.69306081
H_{Al}	-241.13011823	-6.70015381
H_{Fe}	-239.87193998	-9.84197556
$H_{int.}$	-244.31006571	-6.03010129
$H_{Al}\&V_{Al}$	-236.45880203	-2.96779496
$H_{Al}\&V_{Al}$	-234.11641838	-3.996603135
$H_{Fe}\&V_{Al}$	-236.39427834	-5.135533115
$H_{Fe}\&V_{Fe}$	-231.68978914	-4.983288515
$H_{int.}\&V_{Fe}$	-241.38242385	-3.476229715
$H_{int.}\&V_{Fe}$	-238.91325815	-4.441646865

We see that indeed, defects do like to form in the GB, since all the cases favor the formation indicated by the negative sign. Vacancies of both Al and Fe can be expected to be found in an undoped material regularly, as is to be expected, generally more so in Fe positions. Interstitial hydrogen can also be encountered once the material has been subjected to water vapour.

In the presence of vacancies, however, the hydrogen seems to favour filling the vacancy as seen in the largest changes of energy in the cases of replacing Al or Fe with H. Afterwards however, the defects seem to form slightly less likely than from pristine GB. Same with the pristine hydrogen.

The question of more than one hydrogen defect remains. Even if the vacancies do not form to make space, there still might be more hydrogen forming. I consider pursuing this the next logical step after the results of this study to uncover the mechanism of hydrogen embrittlement.

4.3 Cohesive energy

Cohesive energy is the average energy required to remove a particle from the system. If the system is stable, its sign is negative, meaning that it takes work to remove particles.

In the case of an unstable systems the sign turns positive.

The formula for the cohesive energy is rather straightforward. One takes the energy of the full system, then subtracts the constituents and divides by the amount of all the particles. So in our case it is:

$$E_c = \frac{E_{GB} - aE_{Al} - bE_{Fe} - cE_H}{a + b + c}. \tag{4.2}$$

The E_{GB} stands for the total energy of our GB structure model acquired straight from the calculations. The a b and c are the amounts of the particles in question. Their single point energies $E_{Al/Fe/H}$ are calculated by putting the singular atom in an empty cell where it cannot interact or form bonds and then calculating the total energy. These are plotted here:

Particle	Single atom energy(eV)
Al	-0.26486364
Fe	-3.35619009
H	-1.11110154

Finally using the total energies as in the table of formation energies we get the cohesive energies:

Structure	Cohesive energy(eV)
Pristine	-4.145053438
Al vacancy	-4.303207657
Fe vacancy	-4.271830472
Al-H replacement	-4.196570143
Fe-H replacement	-4.242398848
Interstitial H	-4.165314380
Al-H & Al-vac.	-4.191188543
Al-H & Fe-vac.	-4.210392204
Fe-H & Al-vac.	-4.268798870
Fe-H & Fe-vac.	-4.227435723
Int.H & Al-vac.	-4.202877784
Int.H & Fe-vac.	-4.218431802

All of the defects and their combinations made the GB more stable. Singular vacancies seem to make the system more durable than any other types of defects. The more stable vacancy of the two is the Al positioned one. The replacements with H were less stable than the vacancies, but the defects which generally stregthened the GB the least were those of interstitial H. The most stable defect combination was Al vacancy with Fe-H replacement. According to these methods, it can be said that vacancies in the positions of Al and hydrogen in the position of Fe generally make the system most stable.

The embrittlement what we expected to see is not present at all in the face of this method at the least. The observed macroscopic embrittlement can be thought out be due to bigger complexes of defects not discussed in this thesis.

4.4 Density of states

To acquire knowledge of the system's electronic structure; which electrons from which orbitals form the bonds between atoms, the density of states (DOS) for each system has been calculated and plotted. The properties of a matter are due to the electronic structure. This also holds true for our main focus; the strength of the structure. [12] We shall see, if there are trends contributing to the cohesive energy and how the added H will adjust itself in the structure. DOS is calculated in VASP as [13]:

$$\bar{n}\left(\epsilon_i\right) = \frac{N\left(\epsilon_i\right) - N\left(\epsilon_{i-1}\right)}{\Delta\epsilon}. \tag{4.3}$$

Here $\Delta\epsilon$ is the difference between the two energies. The integrated DOS $N\left(\epsilon_i\right)$ is acquired from the electron density $n\left(\epsilon\right)$ so that the total number of electrons are conserved:

$$N\left(\epsilon_i\right) = \int_{-\infty}^{\epsilon_i} n\left(\epsilon\right) d\epsilon. \tag{4.4}$$

4.4.1 Pristine GB

First we shall take a deeper look into the DOS of the pristine case and then note the differences made by the defects.

We define the zero of the energy to be the Fermi energy. DOS in our case is given by the amount of bonding electrons for a given energy (eV). Electrons with upwards spin will be shown as positive and downwards negative.

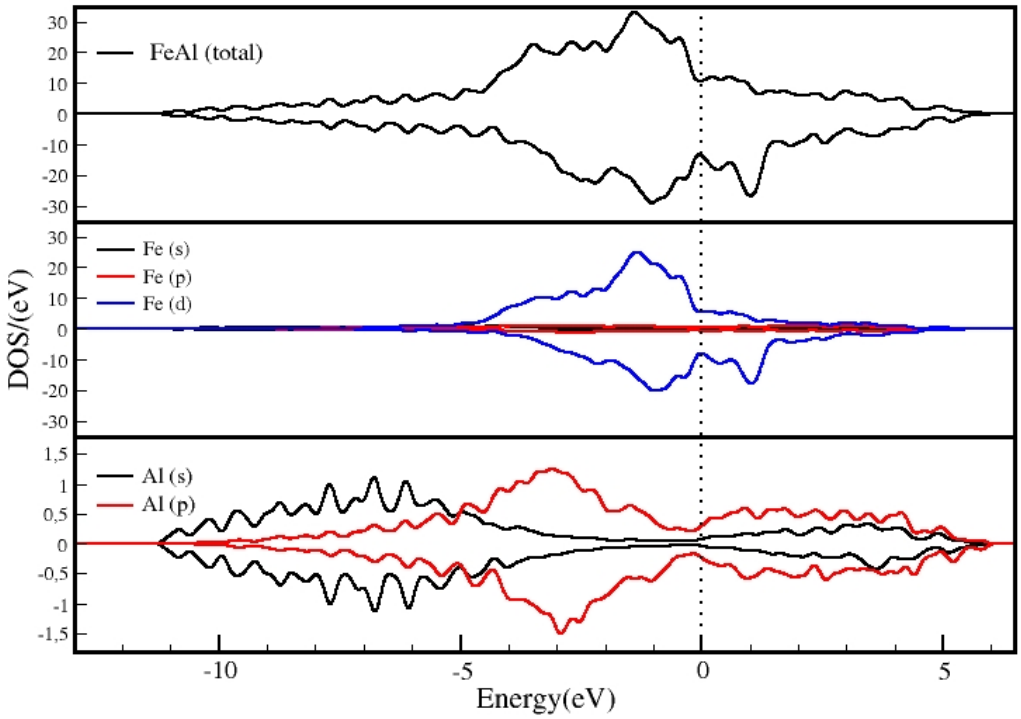

Figure 6: The TDOS and PDOS of the pristine GB by atom type

From the total DOS in the figure 6 we can see that the GB has bonding electrons at the Fermi level, making it metallic as are constituents Fe and Al. S-, p- and d-orbitals of Fe as well as s- and p-orbitals of Al are taking part in the bonding. By far most of the electrons used in bonding come from the d-orbital of Fe. Al has much fewer bonding electrons compared to Fe. All the electrons that contribute can be found in the energy range [-11.5eV, 6.0eV]. The peaks of DOS are mostly in the bonding region (negative area of the x-axis), the largest of which, the Fe-d orbital spike, is next to the Fermi level. The Fe-d orbital playing a big part in bonding as expected in the case of a transition metal such as Fe. All of the cases have bonding electrons near the Fermi level, making all of the GB:s metallic in nature.

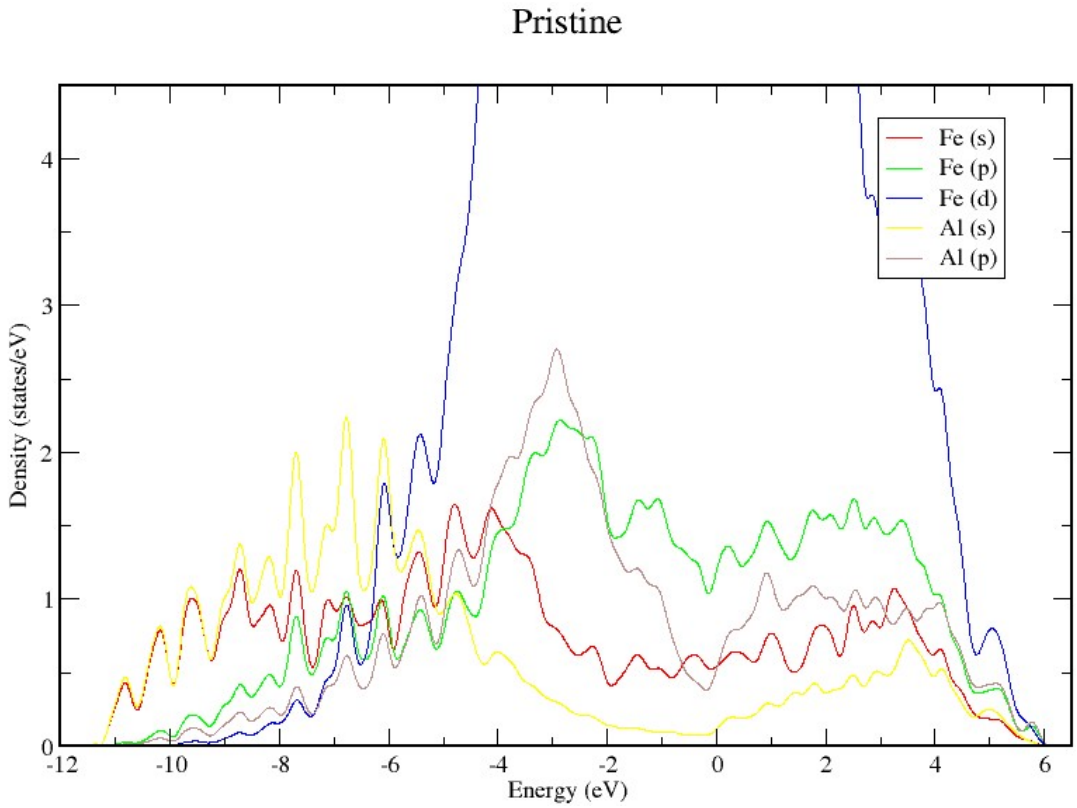

Figure 7: The PDOS of the pristine GB

Moving into the effects of defects, our aim is to look for changes that contribute to the strength of the structure. The main change being the increase of the covalent character of our system by increased hybridisation between the observed orbitals. [12] This can be seen as similar fluctuations on the graph between different kinds of orbitals (s-p, p-d). This can change with added defects. Let us now plot DOS again in a form in which hybridisation can be observed more easily. Let us plot both orbital spins in the same direction and change the scale of the plotting while plotting all the orbitals in the same graph. We get the figure 7. We can now see correlations between s and p orbitals in the energy region -10, -4, after which the common fluctuations seem to subside when the Fe-d spikes up. Some correlation with Fe-d and p orbitals can also be noted, especially with Al-p. Overall the structure indeed has some covalent properties.

4.4.2 Vacancies

Let us first observe the effect of defects in the GB. Two vacancies were introduced to the grain boundary; those of Al and Fe. Subtle changes did indeed happen and the cases

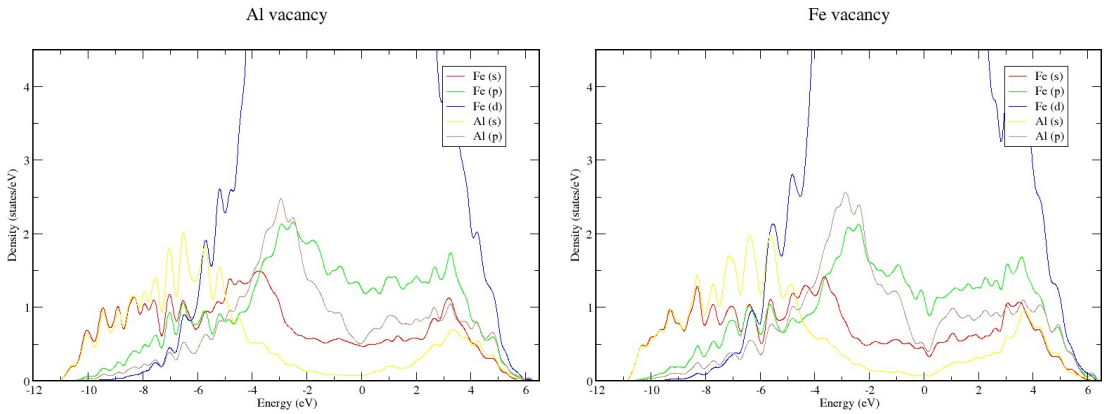

Figure 8: The PDOS of the GB:s with vacancies

do differ as seen in the figure 8. The Al vacancy is showing more hybridisation, than its Fe counterpart and therefore could explain its cohesive energy being lower, and being more stable. The effects of defects can be maybe shown more clearly with the addition of hydrogen.

4.4.3 Hydrogen

In figure 9 the s-orbital of the added hydrogen can act differently depending on its environment. Additional peaks in the bonding region are observed in the case of Fe-H replacement. These additional peaks can be considered to increase the s-p hybridisation and therefore increase bond strength [12], as noted by the cohesive energy. In the case of H-Al replacement the hydrogen aligns itself with the characteristics of the p-orbitals. There are still increase of peaks in the bonding region and the bonding strengthens. This is also the case with the interstitial H, however not as many peaks are observed.

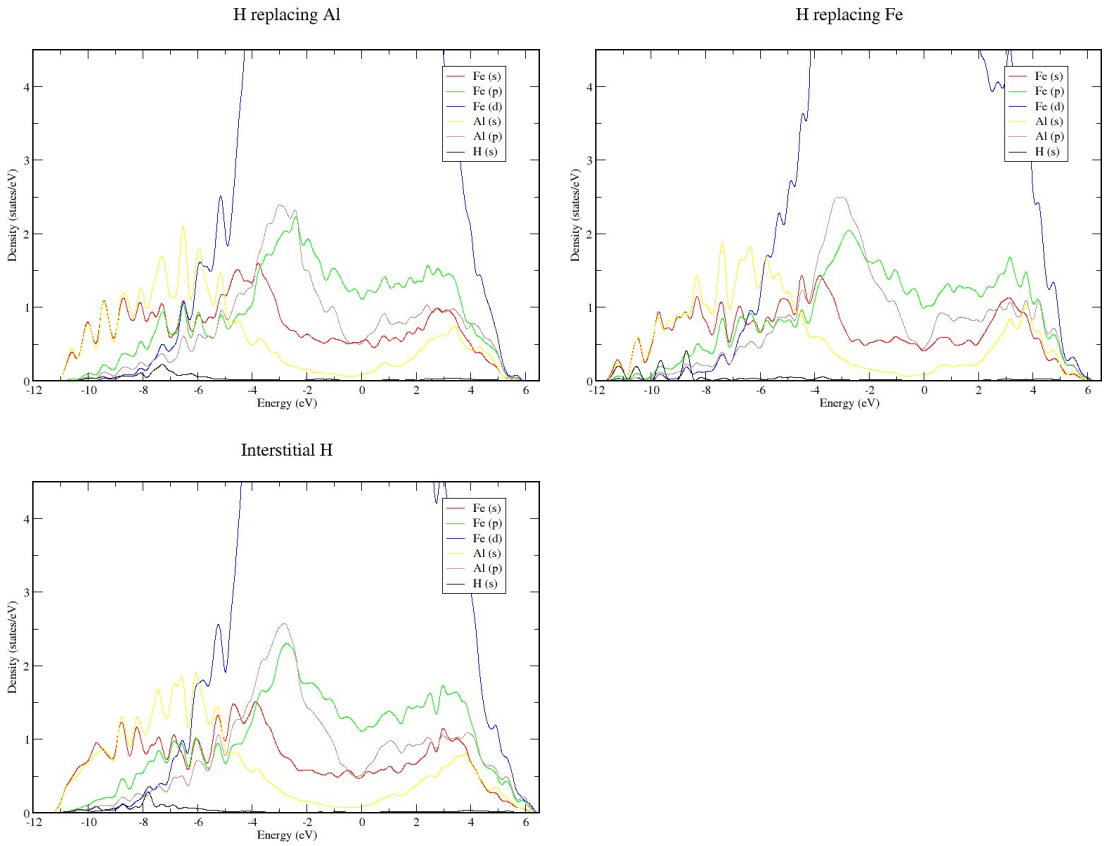

Figure 9: The PDOS of the GB:s with hydrogen

4.4.4 Hydrogen with defects

Here we shall look at the interplay between the hydrogen and the vacancies by looking what effects the vacancies have on the graphs of hydrogen defects. In the case of H-Al replacement and vacancies the hydrogen shows very different kind of behavior depending on the vacancy as seen in the figure 10. With Al vacancy it seems to behave similarly to the p-orbitals and with Fe vacancy a familiar pattern of s-orbital emerges. This s-orbital is less well defined than in the case of just Fe-H replacement, but its presence can explain the increased stability compared to Al vacancy. H-Fe replacements showed themselves to be more stable, than that of Al. With vacancies introduced as well with the H-Fe replacements, all the hydrogens show the familiar s orbital structure. This further supports the claim that this kind of orbital structure can be taken to be stabilising the GB. Interstitial hydrogen was found to strengthen the GB the least. Its vacancy variants however were found to be as stable as the H-Al replacement vacancy variants. The explanation for this can again be found in the s-orbital structure of hydrogen.

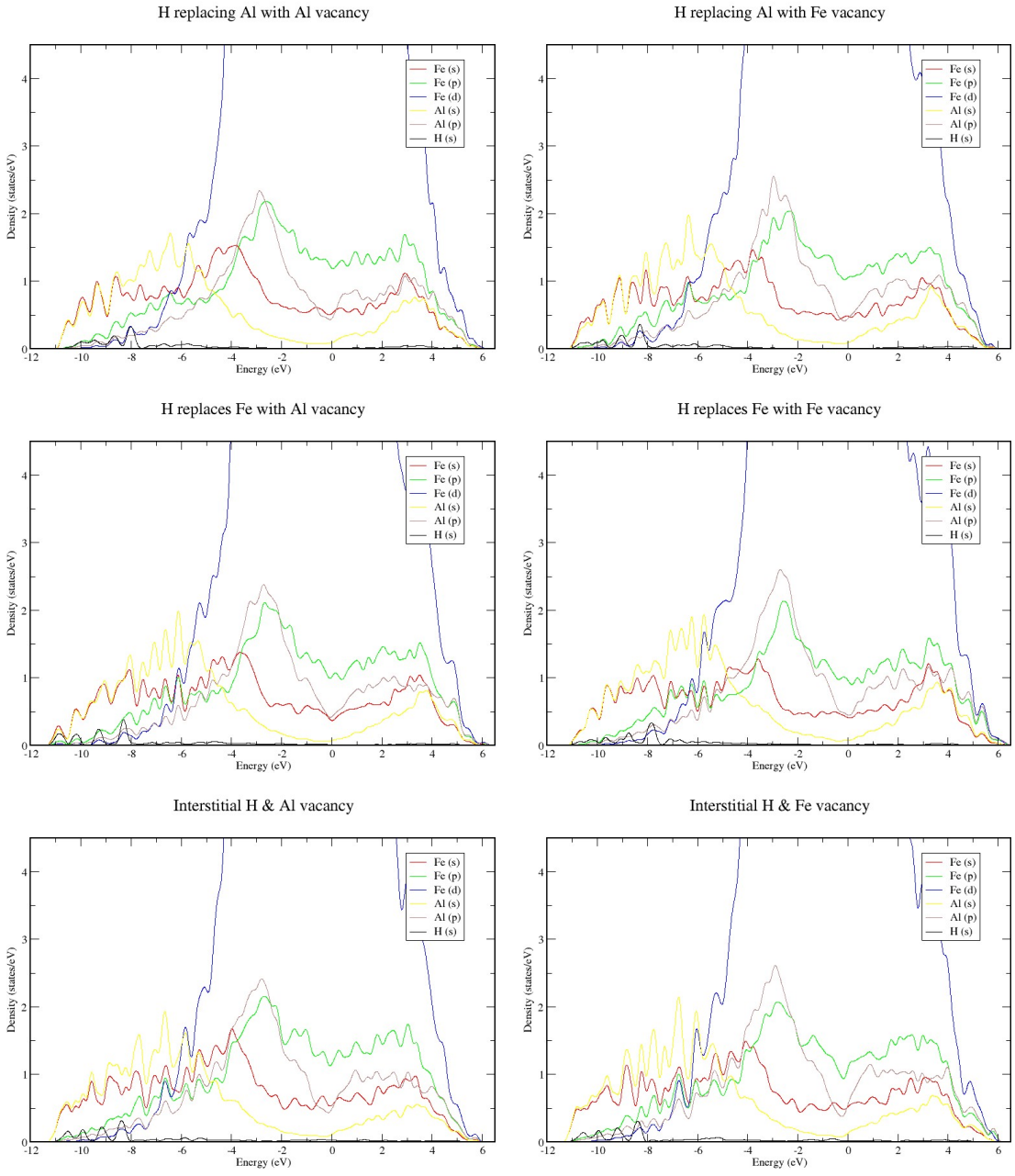

Figure 10: The PDOS of the GB:s with hydrogen and vacancies

5 Conclusions

In this thesis the the formation and effects of point defects were studied by the means of ab-initio simulations in the $\Sigma 5$ grain boundary of FeAl. VASP software was used in all the calculations of this thesis.

The structure was first relaxed to be more like its natural counterpart. The total energy of the structure converged neatly and the movements of four particles were recorded. Surrounding the grain boundary, ring like patterns of Al were observed.

After the relaxation, defects were introduced to the structure. The favorability of defect formation was calculated using the method of formation energies. Defects do indeed like to form in the grain boundary. The most favourable defects were those of hydrogen, the most favorable of them being that of Fe-H replacement. Vacancies do not inhibit the formation of hydrogen.

The strength of the structure was increased in the sense of cohesive energies with added defects in each case. Generally the vacancies in the place of Al and hydrogen in the place of Fe made the structure more stable.

A common factor with the highest stability structures with hydrogen was found in the electronic density of states: a correlation between the singular orbital of H aligning itself with the other s-orbitals and cohesive energy.

As all the defects increased the strength of the structure, we can conclude that singular point defects do not embrittle the grain boundary. The reason for the structural failure can still be due to larger complexes of defects.

References

[1] *Vienna Ab Initio Simulation Package* Official website: www.vasp.at

[2] Ian Baker *An Overview of the Mechanical Properties of FeAl* MRS Online Proceeding Library Archive, January 2011

[3] W. Kohn *Nobel Lecture: Electronic structure of matterwave functions and density functionals* Reviews of Modern Physics, Vol. 71, No. 5, October 1999

[4] J. P. Perdew et al *Generalized gradient approxima-tion made simple* Physical review letters 77, 3865 (1996)

[5] D. Vanderbilt *Soft self-consistent pseudopotentials in a generalized eigenvalue formalism* Physical Review B 41, 7892 (1990)

[6] P. E. Blöchl *Projector augmented-wave method* Physical Review B 50, 17953 (1994)

[7] Hendrik J. Monkhorst and James D. Pack *Special points for Brillouin-zone integrations* Physical review B 13, 5188 (1976)

[8] W. H. Press, B. P. Flannery, S. A. Teukolsky, and W. T. Vetterling *Numerical Recipes* Cambridge University Press, New York, (1986)

[9] M. Methfessel and A. Paxton *High-precision sampling for Brillouin-zone integration in metals* Physical Review B 40, 3616 (1989)

[10] A. F. Kohan, G. Ceder, and D. Morgan *First-principles study of native point defects in ZnO* Physical review B volume 61, number 22, 1 JUNE 2000-II

[11] Neil W. Ashcroft and N. David Mermin *Solid State Physics* Chapters 5 20, College edition (1976)

[12] Chen Yu, Yao Zheng-Jun, Zhang Ping-Ze and Luo Xi-Xi *Effects of a vacancy, Cr and Mo on the electronic structure of FeAl3* $(10\bar{1})$ *[111] grain boundaries* Materials Research Express, Volume 6, Issue 2, article id. 026514 (2019)

[13] *VASP wiki: DOSCAR*

In literature review:

[14] Gang Lu and Nicholas Kioussis *Interaction of vacancies with a grain boundary in aluminum: A first-principles study* PHYSICAL REVIEW B, VOLUME 64, 02410

[15] J. M. Raulot, A. Fraczkiewicz, T. Cordonnier, H. Aourag and T. Grosdidier *Atomistic study of the effect of B addition in the FeAl compound* Journal of Materials Science, June 2008

[16] Z. R. Xu R. B. McLellan
The thermodynamics and solubility of hydrogen in FeAl
Journal of Physics and Chemistry of Solids, Volume 61, Issue 4, p. 633-635.

[17] Guikai Zhang, Guangqi Huang, Meijuan Hu, Feilong Yang, Lang Liu, Jürgen Konys and Tao Tang
Stability and clusterization of hydrogen-vacancy complexes in B2-FeAl: insight from hydrogen embrittlement
RSC Adv., 2017, 7, 11094

[18] Sutatch Ratanaphan, David L. Olmsted, Vasily V. Bulatov, Elizabeth A. Holm, Anthony D. Rollett and Gregory S. Rohrer
Grain boundary energies in body-centered cubic metals
Acta Materialia 88 (2015) 346354

[19] Miroslav Čák, Mojmír Šob and Jürgen Hafner
First-principles study of magnetism at grain boundaries in iron and nickel PHYSICAL REVIEW B 78, 054418 (2008)

[20] E. Wachowicz, T. Ossowski, and A. Kiejna
Cohesive and magnetic properties of grain boundaries in bcc Fe with Cr additions
PHYSICAL REVIEW B 81, 094104 (2010)

[21] S. Gialanella, R.S. Brusa, W. Deng, F. Marino, T. Spataru and G. Principi
Defect structures in FeAl B2 alloys
Journal of Alloys and Compounds 317318 (2001) 485490

[22] Ian M. Robertson, P. Sofronis, A. Nagao, M.L. Martin, S. Wang, D.W. Gross, and K.E. Nygren
Hydrogen Embrittlement Understood
2014 Edward DeMille Campbell Memorial Lecture ASM Internatinal

[23] MSE 5317; Computational materials science
Hydrogen Embrittlement of Metals
http://electronicstructure.wikidot.com/hydrogen-embrittlement-of-metals